



Bulletin of the Mineral Research and Exploration

<http://bulletin.mta.gov.tr>



Analysis of the stress distribution of North Anatolian Fault Zone for the part between Amasya-Tokat cities

Ayça ÇIRMIK^{a*}, Ufuk AYDIN^b, Oya ANKAYA PAMUKÇU^a and Fikret DOĞRU^c

^aDokuz Eylül University, Faculty of Engineering, Department of Geophysical Engineering, İzmir, Türkiye

^bAtatürk University, Faculty of Engineering, Department of Civil Engineering, Erzurum, Türkiye

^cAtatürk University, Oltu Vocational Collage, Construction, Erzurum, Türkiye

Research Article

Keywords:

GNSS, Regional Absorption Coefficient, Coulomb Stress / Strain Analysis.

ABSTRACT

Tectonic forces formed in the continental crust, cause permanent changes in stress, compression and deformation. The amplitudes of earthquake waves vary with the stress/strain distribution in the crust. In this study, the change of stress/strain and regional absorption coefficient, which is effective in tectonic forces caused by elastic deformation energy accumulating in the brittle crust over time, was investigated. The study area is the middle part of the North Anatolian Fault Zone and the area formed by Ezinepazarı fault zone and Merzifon fault zone. In this area, Coulomb stress analysis was carried out by using the focal mechanism solution values of the earthquake that occurred in Yoldere - Erbaa, Tokat on October 9, 2015 ($M_L=5.1$). In order to examine the deformation caused by this earthquake in and around the study area, Global Navigation Satellite System (GNSS) data were evaluated and the velocities of these stations were calculated using GNSS data of these stations for the years 2013-2014-2015-2016. Also, regional absorption coefficients were determined by using earthquake data. As a result, Coulomb stress analysis results, velocity values distribution obtained from GNSS data and absorption findings obtained from seismological study were evaluated together.

Received Date: 01.07.2021

Accepted Date: 02.11.2021

1. Introduction

The internal force fields that cause the distortion in the bodies can be approximately estimated based on the deformation generated by the displacement of the blocks during an earthquake. The kinematics of continental deformation are shown by the horizontal and vertical variation amounts derived by monitoring the temporal changes of the coordinates, which allow an estimate of the internal stress/strain amount in the tectonic forces of such deformation. Increasing of the effective stresses causes stresses, thus earthquakes in the deformed areas of the fault zone (Chinnery,

1963). Many researchers have investigated Coulomb stress variation (Harris and Simpson, 1992; Stein et al., 1992; Çırmık, 2014; Çırmık et al., 2016; Çırmık and Pamukçu, 2017; Çırmık et al., 2017; Affandi et al., 2019). Changes in stress or strain in the crust affect not just the velocity of seismic waves created during the earthquake, but also the amplitudes of those waves. There are numerous factors that affect seismic absorption in the crust, and changing conditions have a major impact (Toksöz and Johnston, 1981). The lithological structure and stress/strain state of the environment influence the absorption of earthquake

Citation Info: Çırmık, A., Aydın, U., Pamukçu A. O., Doğru, F. 2022. Analysis of the stress distribution of North Anatolian Fault Zone for the part between Amasya-Tokat cities. Bulletin of the Mineral Research and Exploration 169, 121-133. <https://doi.org/10.19111/bulletinofmre.1022323>

*Corresponding author: Ayça ÇIRMIK, ayca.cirmik@deu.edu.tr

energy that causes continental crust deformation in the time-distance environment (reduction in wave amplitude - increase). The rate of decrease in the wave amplitude gives a good idea of the absorption (Aki, 1969). In our country and around the world, many studies on absorption have been undertaken (Aki and Chouet, 1975; Aydın and Kadirov, 2008; Ugalde et al., 2010; Aydın, 2014, 2016). Pamukçu et al. (2015) investigated vertical mass movements in the south of İzmir. Furthermore, using the Coulomb software (Toda et al., 2011), Çırmık et al. (2017) studied the kinematic structure of the Gülbahçe fault. The impact area of the earthquakes nearest to the region was calculated initially in this context. Then, using the software Gamit/Globok (Herring et al., 2015), the GNSS data of Continuously Operating Reference Stations (CORS-TR) and the probable velocity structure in the region was estimated.

Within the context of this study, stress and strain distributions were calculated in Amasya-Tokat provinces and the surrounding region, and absorption analysis was undertaken for the same region. The relationship between the absorption study results and the Coulomb stress variation within the crust was investigated, and the seismicity was compared.

2. Tectonics of the Study Area

Seismic activity in Anatolia, the North Anatolian Fault Zone (NAFZ), the Aegean Graben System (AGS), the East Anatolian Fault Zone (EAFZ), the East Anatolian Compression Zone, the Hellenic Cyprus Arc, and the Central Anatolian Plain Region, six basic seismic regimes are used to express it. From the Saros Gulf to Karlıova, the NAFZ is around 1200 kilometers long (Figure 1). The NAFZ (Ketin, 1948; Şengör, 1979; Şengör and Natal'in, 1996; Şengör et al., 2005) is one of the world's most active strike-slip faults. The NAFZ connects the Aegean Taphrogene with the Eastern Anatolian High Plateau and extends parallel to the Black Sea for about 100 kilometers (Taymaz et al., 1991; Koçyiğit et al., 2001; Şengör et al., 2005). The Ezinepazarı fault (Şaroğlu et al., 1987) is a 250-kilometer-long fault that originates in the NAFZ and continues southwest through the Ezinepazarı, Amasya, and Sungurlu districts, ending

near Delice (Şaroğlu et al., 1987). The Merzifon fault is a 30-kilometer-long E-W directional fault that runs along the Merzifon plain from the south (Arpat and Şaroğlu, 1975; Şaroğlu et al., 1987) (Figure 1)

3. Method

3.1. Coulomb Analysis

Coulomb v3.3 software (Toda et al., 2011) is used to calculate displacement, stress, and strain at any depth caused by faults. Calculations in this software are performed in an elastic half-space environment containing the uniform, isotropic elastic properties specified by Okada (1992). In the Coulomb criterion, if the Coulomb stress (σ_f) exceeds a certain value, the collapse that occurs on a surface is indicated by the following equation:

$$\sigma_f = \tau_\beta - \mu (\sigma_\beta - p) \quad (1)$$

The shear stress at the failure surface is τ_β , the normal stress is σ_β , the pore water pressure is p , and the friction coefficient is μ (Toda et al., 2011).

As a result, the overall effect of the shear stress and the normal stress change values equal the Coulomb stress variation estimated for a medium.

3.2. Absorption Analysis

The method of decay of seismic wave amplitudes overtime was utilized to find out the regional absorption coefficient. The following formula is used to calculate the amplitude decrease (absorption) (Aki and Richards, 1980),

$$A(x, t) = A_0^{i(kx-wt)} \quad (2)$$

Where A_0 ; $x=0$ represents the amplitude (focal amplitude) at time $t=0$ and distance $x=0$, w is the angular frequency, and k is the number of waves. Absorption can be defined in terms of frequency or number of complex waves (Toksöz and Johnston, 1981).

The logarithm of the decrease in the amplitude of the harmonic wave expresses the absorption of the medium. A_{x_1} ; the amplitude at x_1 distance, A_{x_2} the amplitude at x_2 distance and ($x_1 > x_2$), the absorption

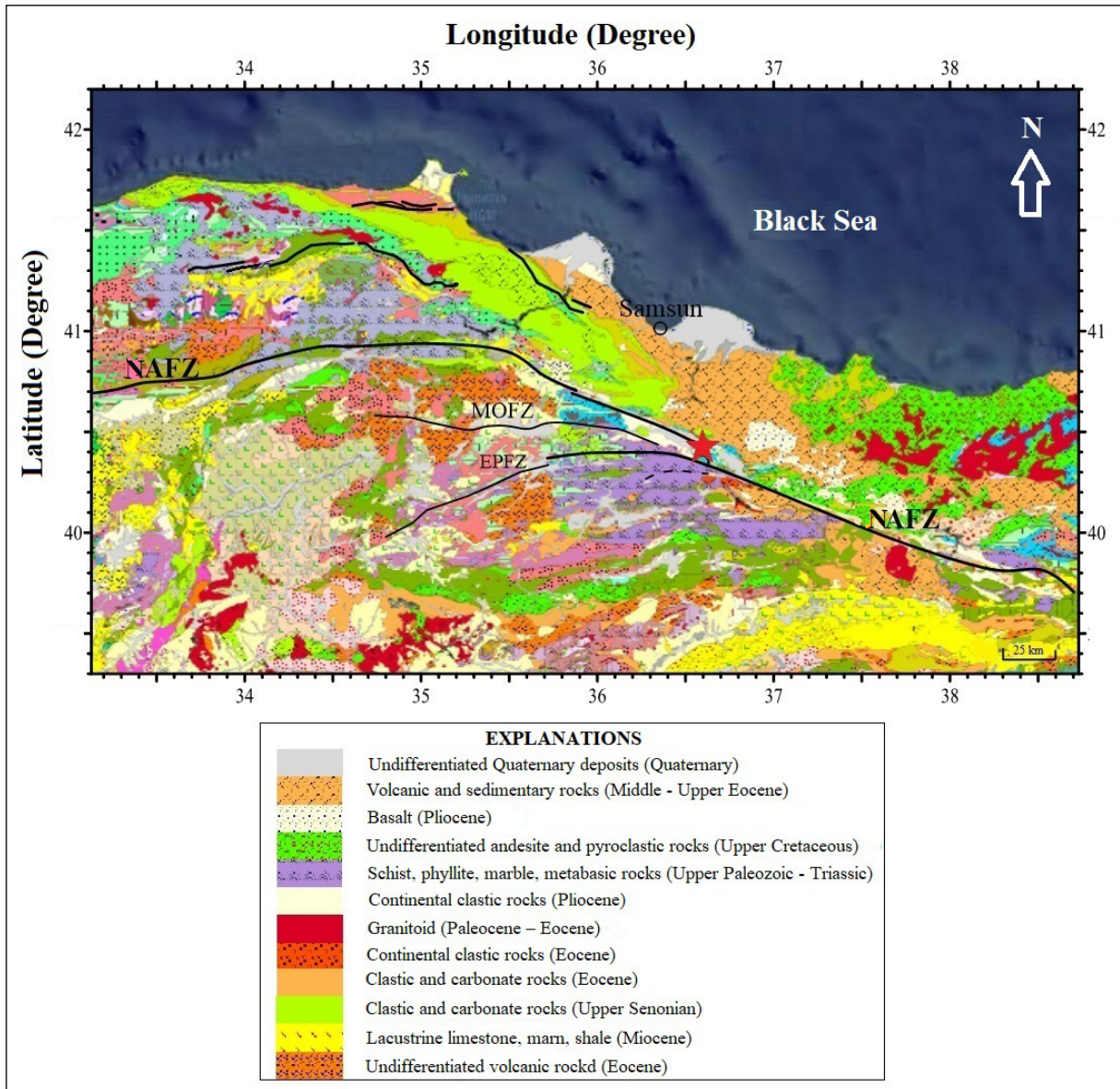


Figure 1- General tectonic and geological structure of the study region and its surroundings (modified from <http://yerbilimleri.mta.gov.tr/anasayfa.aspx>). NAFZ: The North Anatolian Fault Zone, MOFZ: Merzifon Ovacık Fault Zone, EPFZ: Ezinepazarı Fault Zone. The red star represents the epicenter of the earthquake that occurred on October 9th, 2015 ($M_L=5.1$).

coefficient (Chopra and Alexeev, 2004) is defined as follows.

$$\delta = \frac{1}{x_2 - x_1} \ln \left(\frac{A(x_1)}{A(x_2)} \right) \quad (3)$$

$$A_x = A_0 e^{-\delta x} \quad (4)$$

4. Data and Findings

An earthquake with a magnitude of $M_L=5.1$ and a focal depth of roughly 5 km occurred near Yoldere - Erbaa (Tokat) on 09 October 2015, according to data

from the Boğaziçi University Kandilli Observatory Earthquake Research Institute (KOERI, 2015). According to the KOERI's estimated intensity map, the intensity value was $I_0=V$ in the epicenter (Erbaa) and $I_0=IV$ in Tokat province. The earthquake epicenter is located over the NAFZ. The largest earthquake in the region since 1900 ($M = 7.0$) struck Erbaa - Tokat on December 20, 1942 (KOERI, 2015). The stress and strain values caused by the 9 October 2015 Yoldere - Erbaa (Tokat) ($M_L = 5.1$) earthquake were computed

by Coulomb v3.3 software using the earthquake focal mechanism solution data (Table 1) provided by KOERI (Figure 2, 3).

In the other step of the study, GNSS data belonging to the CORS-TR stations were used to examine the tectonic effects of the earthquake ($M_L=5.1$) that occurred in Yoldere-Erbaa district of Tokat province on 9th October 2015 (Figure 4). 61 days of data from the GNSS stations namely; TOK1 (Tokat, City Center), RDIY (Tokat, Reşadiye), GIRS (Giresun, City Center), FASA (Ordu, Fatsa), SAM1 (Samsun, City Center), VEZI (Samsun, Vezirköprü) and CORU (Çorum, City Center) including 30 days (9th September) before and 30 days (9th November) after earthquake data were evaluated with Gamit/Globk (Herring et al., 2015) software. The process was made by taking the Eurasia plate fixed. The International GNSS Service (IGS) stations; BUCU, GLSV, ISTA,

MATE, MIKL, NICO, PENC, TUBI, and ZECK were chosen, and ITRF 2014 was utilized as the International Terrestrial Reference System (ITRF). Table 2 shows the GNSS data evaluation strategy as well as the GNSS data assessment technique.

The time series (Figure 5) were constructed for the date range corresponding to the 252nd and 313th days, and the date of 9th October 2015, which coincides with the 282nd day of 2015. The Eurasian plate was fixed in the next step of this stage by analyzing the GNSS data of these stations for the years 2013, 2014, 2015, and 2016, as well as their velocities (Figure 6).

Data from the Boğaziçi University Kandilli Observatory, as well as the Ministry of Public Works and Settlement (Ministry of Environment, Urbanization, and Climate Change)'s KVK (Kavak, Samsun), RSDY (Reşadiye, Tokat), and TOKT

Table 1- The source parameters used in the Coulomb v3.3 software (Toda et al., 2011).

Poisson Ratio	Young Module (bar)	Coefficient of Friction	Institute Name	Strike Angle (°)	Dip Angle (°)	Rake Angle (°)	Depth (km)
0.25	8×10^5	0.4	KOERI	280	86	178	5

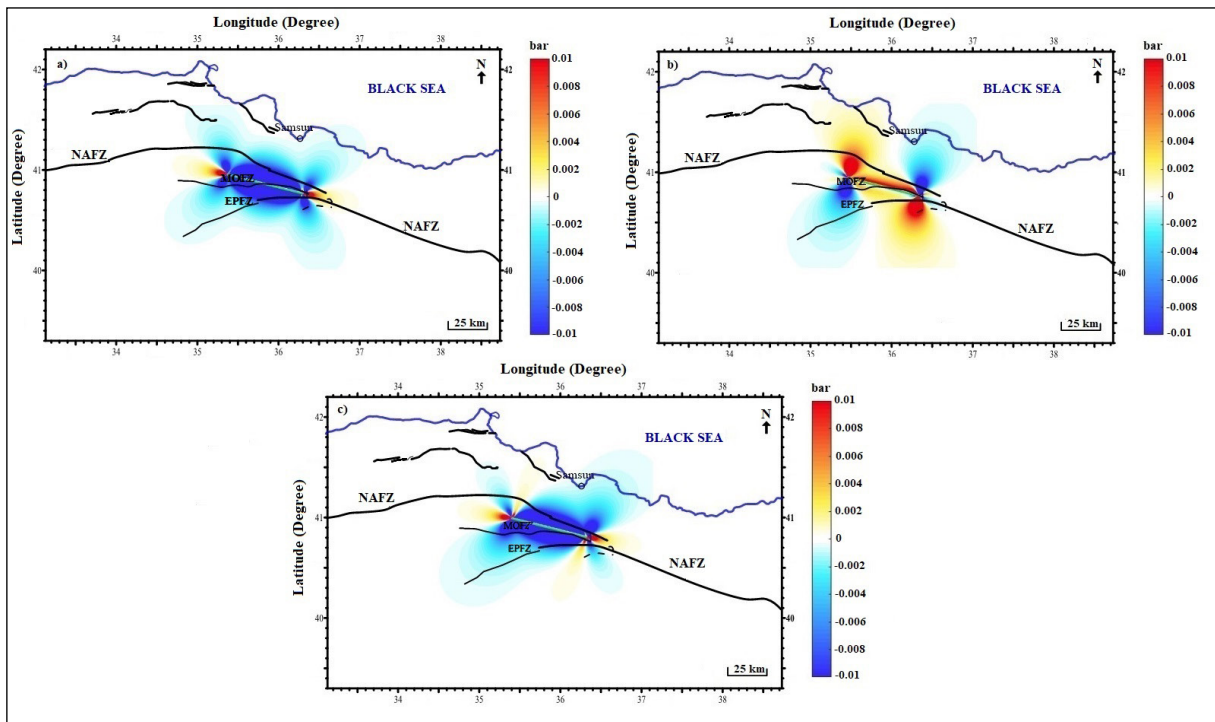


Figure 2- a) Shear stress, b) normal stress, and c) Coulomb stress values calculated by the earthquake focal mechanism data of KOERI (blue color: stress release, red color: stress loading).

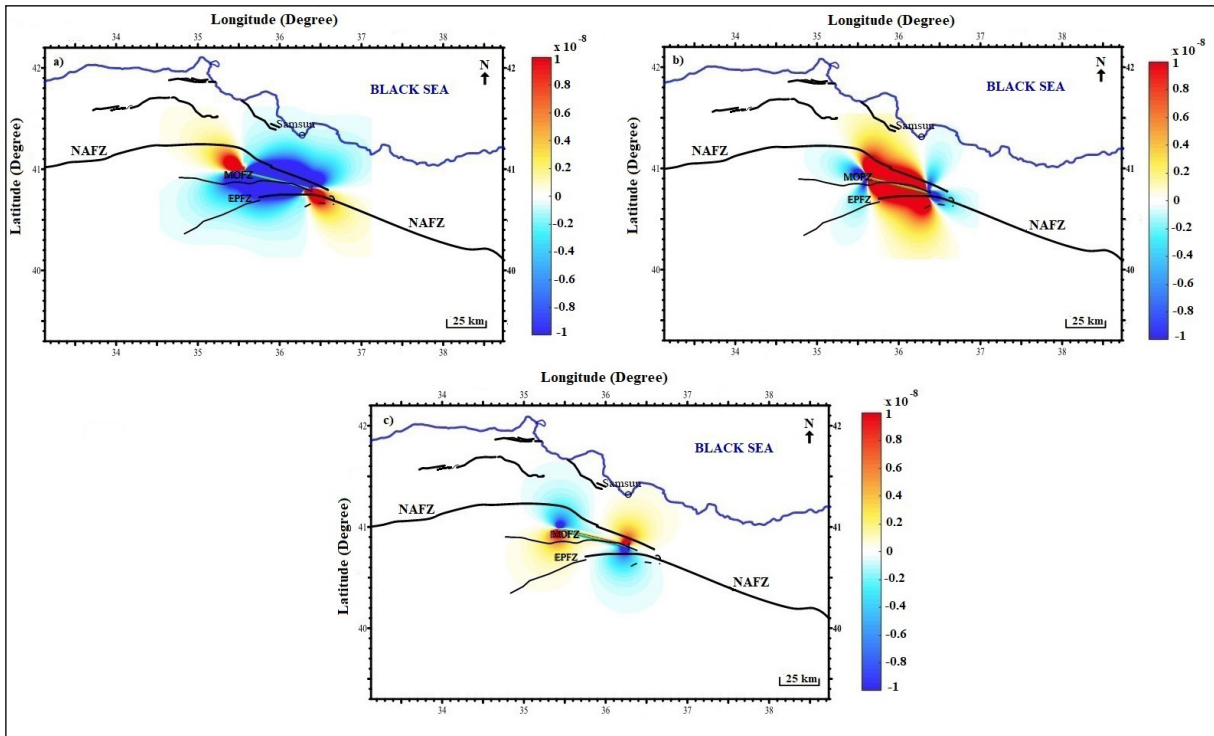


Figure 3- The strain a) XX, b) YY, and c) ZZ component variations calculated by using the earthquake focal mechanism data of KOERI.

Table 2- The processing strategy of GNSS data.

Software	Gamit/Globk Version 10.71
Data range	30 sec./24 hours Daily data
Process days	9 th September – 9 th November 2015 (between 252 th - 313 th days of 2015)
Cut-off angle	10°
Ephemeris Data	IGS final orbital and IGS ERP folders
Antenna Phase Centre Data	The weighted phase center model was associated with the high angle (PCV-antmod.dat).
The parameters of Troposphere	VMF1 (Vienna Mapping Function) was used. Zenith delay parameters were calculated every 2 hours.
International Terrestrial Reference System	ITRF 2014
Stabile Stations	Eurasia fixed reference system was used. BUCU, GLSV, ISTA, MATE, MIKL, NICO, PENC, TUBI, and ZECK stations were chosen as IGS reference stations.
Final Coordinate Calculation	61 days GNSS data were combined with GLOBK.

(Tokat) stations, were used in the absorption analysis (Figure 7). A total of 192 mass wave data from three stations (KVK, RSDY, and TOKT) were used in the study, which included the effects of all three faults in the area (Figure 7). These data were used to calculate the absorption values of Pg and Sg waves (Figure 8). The study included earthquakes with magnitudes ranging from 3 to 5.1 and focal depths ranging from 1.2 to 32 km, with the epicenter distances of

these earthquakes being around 150 km. For each of the three sites, regional absorption values and coefficients of Pg and Sg waves were determined. Figure 8 shows the calculated Pg and Sg absorption values for the earthquakes at the three stations. The regional absorption coefficients were calculated using these values (Table 3) and the regional absorption coefficients' lateral tomography images are presented in Figure 9.

5. Discussion

The evaluation of GNSS data and Coulomb stress/strain calculations in and around the Merzifon Fault and Ezinepazarı Fault zone within the scope of the study region in the NAFZ were done in the first part of this study. It was observed that the amplitude values were generally low in and around the region where the earthquake occurred, based on the stress and strain results (Figure 2) obtained with the Coulomb v3.3 software using the earthquake focal mechanism solutions values (Table 1) specified by KOERI for the Yoldere - Erbaa (Tokat) ($M_L = 5.1$) earthquake on October 9, 2015.

According to the stress analysis results, stress is released in the blue sections and loaded in the red sections in the shear stress (Figure 2a), normal stress (Figure 2b), and Coulomb stress (Figure 2c) variations. In the shear stress values (Figure 2a), it is seen that there is stress loading at the east and west

ends of the fault, where the red color dominates, and stress releases at the northern and southern ends of the fault, where the blue color dominates. According to the normal stress values (Figure 2b), the stress is loaded in the northwest and southeast sections of the fault, and the tension is released in the NE - SW segment. The energy originating from the earthquake generates stress loading at both ends of the fault and stress release in the northern and southern sections of the fault, as seen in the Coulomb stress values which contain the overall effect of shear and normal stress (Figure 2c). In addition, the change values in the strain's XX (Figure 3a), YY (Figure 3b), and ZZ (Figure 3c) components were assessed as part of this study. Negative amplitude strain occurs in the north and south of the fault, while positive amplitude strain occurs at both ends of the fault, according to the XX component of the strain induced by the earthquake (Figure 3a). In the YY component of the strain (Figure 3b), it is seen that negative amplitude values occur

Table 3- The coordinates of the stations and the Pg, Sg regional absorption coefficients.

Station	Longitude (°)	Latitude (°)	Amount	δP_g (km/1)	δS_g (km/1)	$\delta S_g / \delta P_g$	Location
KVK	36.0463	41.0807	60	0.0203	0.0248	1.2216	SAMSUN
RSDY	37.3273	40.3972	57	0.029	0.0238	0.8207	TOKAT
TOKT	36.5445	40.3173	75	0.0106	0.0131	1.2359	TOKAT
TOTAL	-----	-----	192	-----	-----		

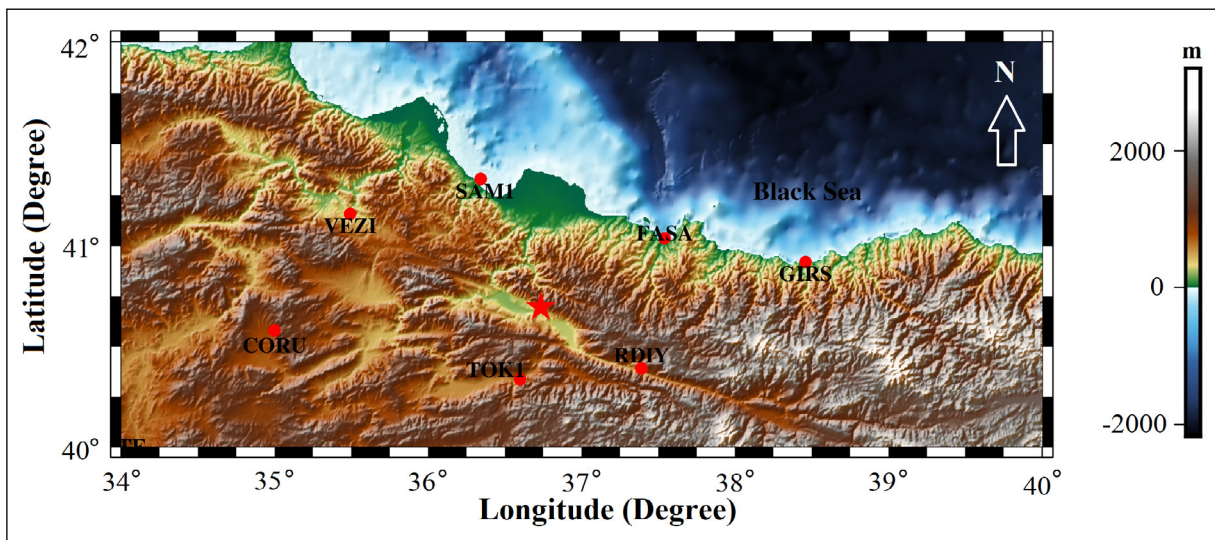


Figure 4- The view of the CORS-TR stations located near the epicenter (Erbaa district of Tokat province) of the 9th October 2015 ($M_L=5.1$). Red dots: the locations of GNSS stations of CORS-TR, red star: the epicenter of the 9th October 2015 ($M_L=5.1$) earthquake.

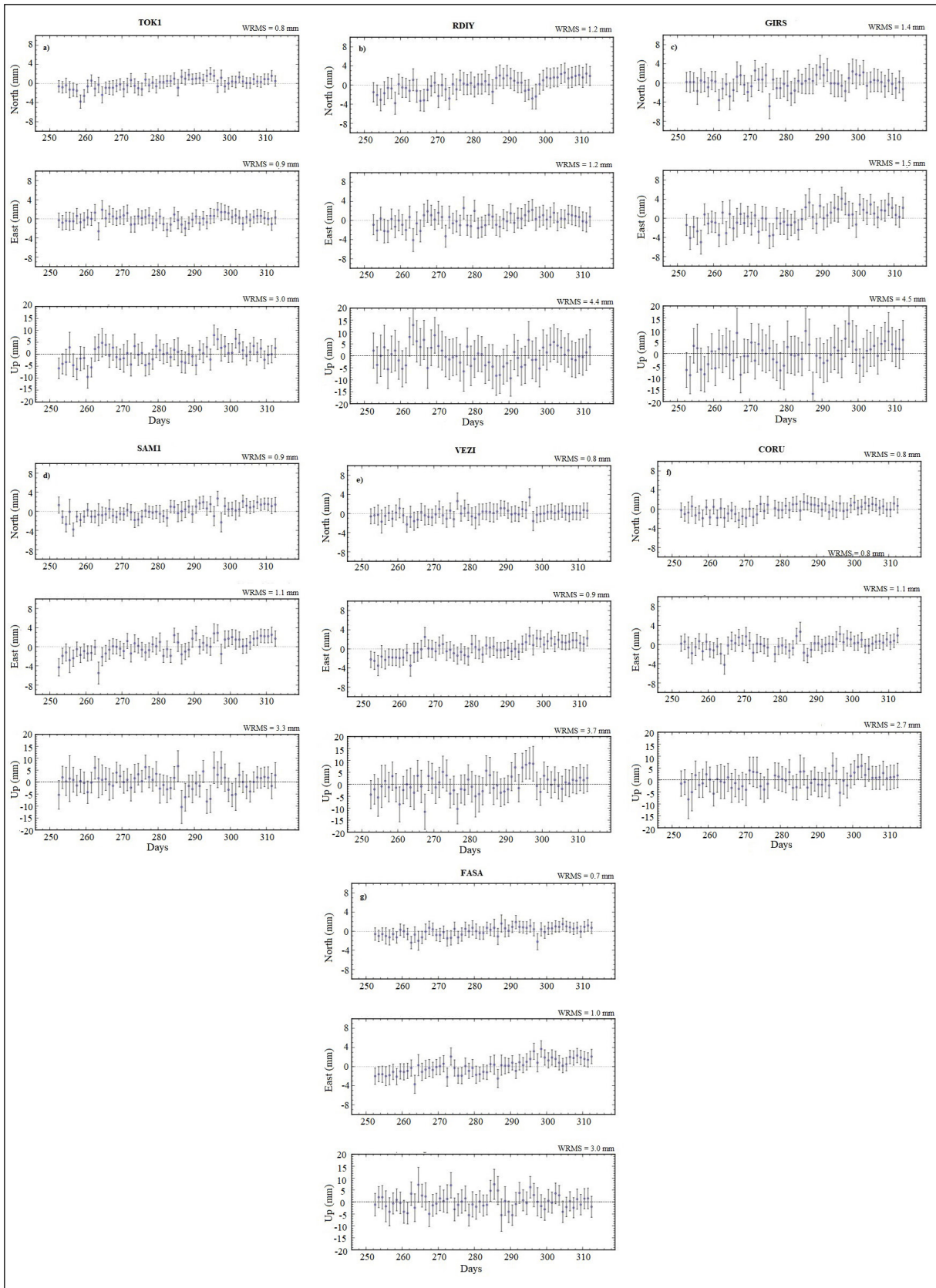


Figure 5- The north, east and up components of the time series for the 252nd - 312th days of 2015 of the stations a) TOK1, b) RDIY, c) GIRS, d) SAM1, e) VEZI, f) CORU, and g) FASA.

at both ends of the fault, whereas positive amplitude values occur in the north and south. In the ZZ component, negative amplitude values occur at both northwestern and southeastern of the fault.

In the other step, the deformation of GNSS stations induced by this earthquake was investigated with the time series (Figure 5). As a general result, it was found that the Yoldere - Erbaa earthquake on 9th October 2015 ($M_L = 5.1$) did not generate significant deformation in the region. However, in the time series of TOK1 (Figure 5a), it is seen that there is a movement at the coseismic period (282th Julien day) at the northern component. A movement was also detected in the eastern component at the CORU (Figure 5f). It can be said that the Tokat - Erbaa earthquake ($M_L=5.1$) caused deformation in the northern component at TOK1 station which is closest to the epicenter. For investigating the reason of the movement at CORU (Figure 5f), which location is not close to the epicenter (Figure 4), the tectonism of this region needs to be studied in detail.

In the other step of the study, the velocities of the GNSS stations were calculated for the years 2013, 2014, 2015, and 2016 (Figure 6). In Figure 6, it is seen that the velocities of SAM1, FASA and GIRS stations were slower than the velocities of VEZI,

CORU, TOK1, and RDIY stations. The directions of the velocity vectors of the stations are towards NW in general. According to the differences in the velocity vector directions, it is seen that the north component of the velocity of CORU is less dominant than the other stations (Figure 6). The velocities of CORU (Çorum, City Center) and TOK1 (Tokat, City Center) are faster than other GNSS stations in the region, as seen in Figure 6. The difference in velocity vector direction at the CORU station can be interpreted as the tectonic structure of the region in which CORU is located is different from the region of TOK1.

According to the findings of the study area, it can be said that the crustal motion is stable. There are two possible explanations for this event. First, an elastic deformation in the study area might be explained by the accumulation of energy or the fact that this area is more rigid than others. Another option is that the data was collected from stations that were relatively unaffected by the earthquake since they were located far from the epicenter. Therefore, GNSS measurements on the bedrock representing the kinematic mechanism should be pre-planned in the study area to determine the underground deformation more precisely and in detail, or continuous GNSS stations should be used to continually monitor this tectonism.

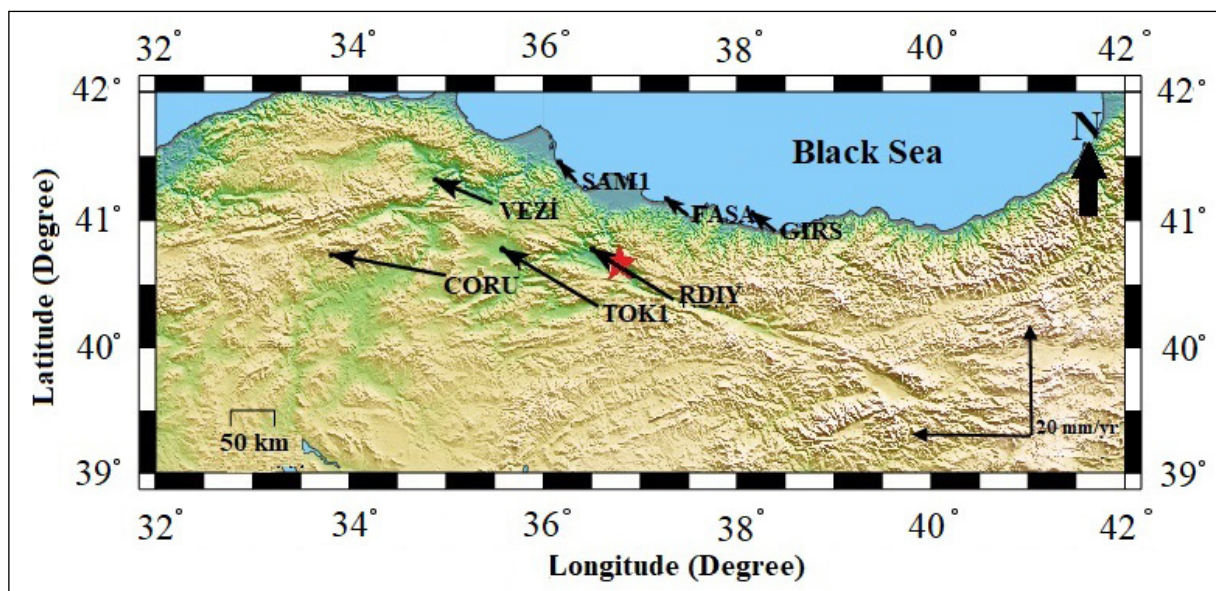


Figure 6- The velocity vectors estimated with the Eurasian plate fixed using GNSS data of CORS - TR stations between the years 2013-2016. The epicenter of the 9th October 2015 ($M_L = 5.1$) earthquake is shown by a red star

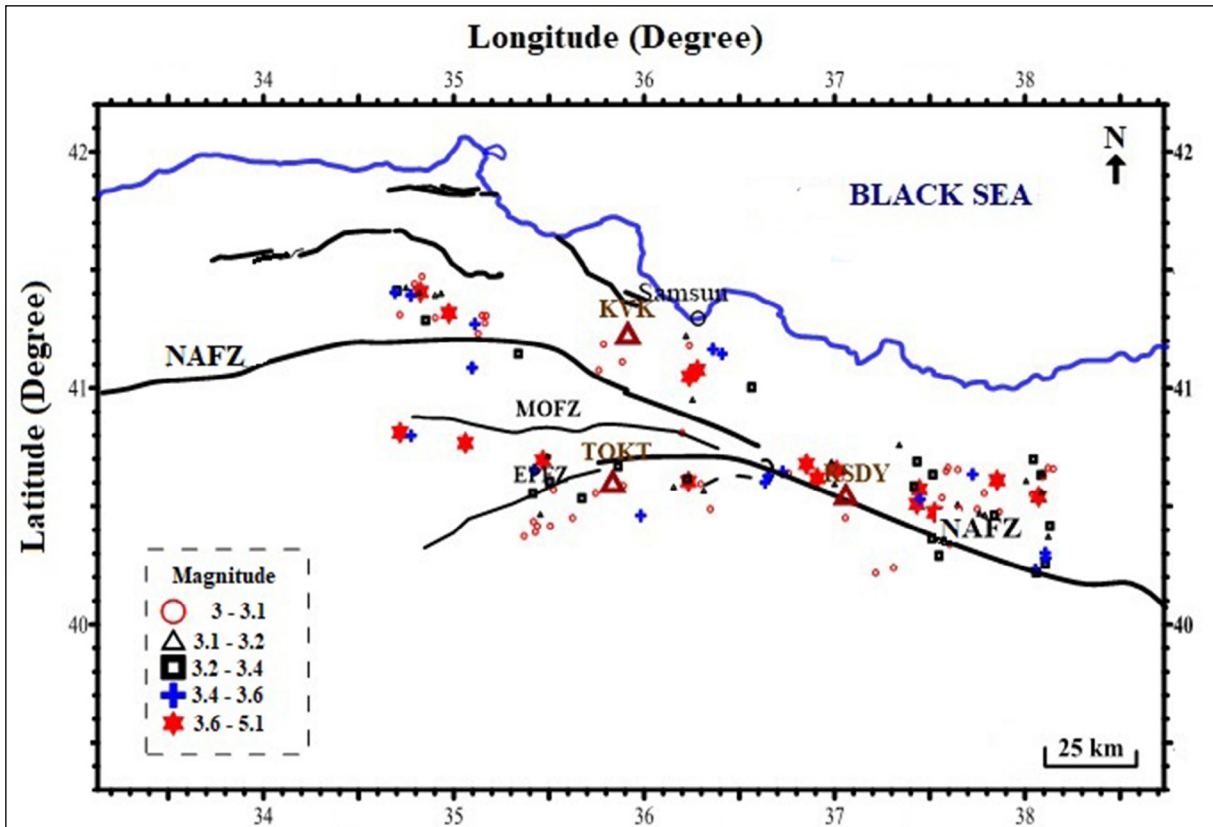


Figure 7- The locations of the stations (KVK, TOKT, RSDY) and the distribution of earthquakes used in the absorption analysis. Burgundy triangles represent the locations of the stations. NAFZ: North Anatolian Fault Zone, MOFZ: Merzifon Ovacık Fault Zone, EPFZ: Ezinepazarı Fault Zone.

Seismic waves are affected not only by the elastic parameters, lithological, and chemical properties of the medium but also by changes in the medium's stress/strain properties (Aydın, 2011). A decrease in absorption is caused by an increase in the underground pressure. One of the elements controlling absorption is pressure and/or stress as the first order (Aydın, 2011). The internal stress/strain distribution and regional absorption variation, which are effective in tectonic forces created by elastic deformation energy accumulating in the brittle crust over time, were explored in another step of the study in light of this knowledge. For KVK, TOKT, and RSDY stations, absorption values (Figure 8) and absorption coefficients (Figure 9) were calculated. The highest P_g and S_g absorption values in the region were obtained from KVK (Figure 8a) and RSDY (Figure 8b) station, whereas TOKT (Figure 8c) station had the lowest absorption values. The regional absorption coefficient (δ_p and δ_s) values in KVK and RSDY stations are

greater than the values in the TOKT station. (Figure 9). The RSDY station has the highest P_g and S_g absorption (Figure 8b) and regional absorption coefficients values (Figure 9a, and 9b). Therefore, it can be said that the crustal structure of RSDY and its surroundings have intense faulting mechanism than the crustal structure of KVK and its surroundings. The reason of lower values of TOKT station (Figure 8 and Figure 9) than others can be explained by the fact that the location of the TOKT is close to the MOFZ and EPFZ, as seen in Figure 9. In addition, the lowest findings (Figure 9) show that TOKT and its surroundings are under more pressure than the other two stations. These findings show that the compression impact is stronger in the region between NAFZ and EPFZ than other regions and lower compression affects Reşadiye (Tokat) and its surroundings.

When the Coulomb stress values obtained from the Coulomb analysis are compared with the locations of the seismology stations used in the study (Figure 10),

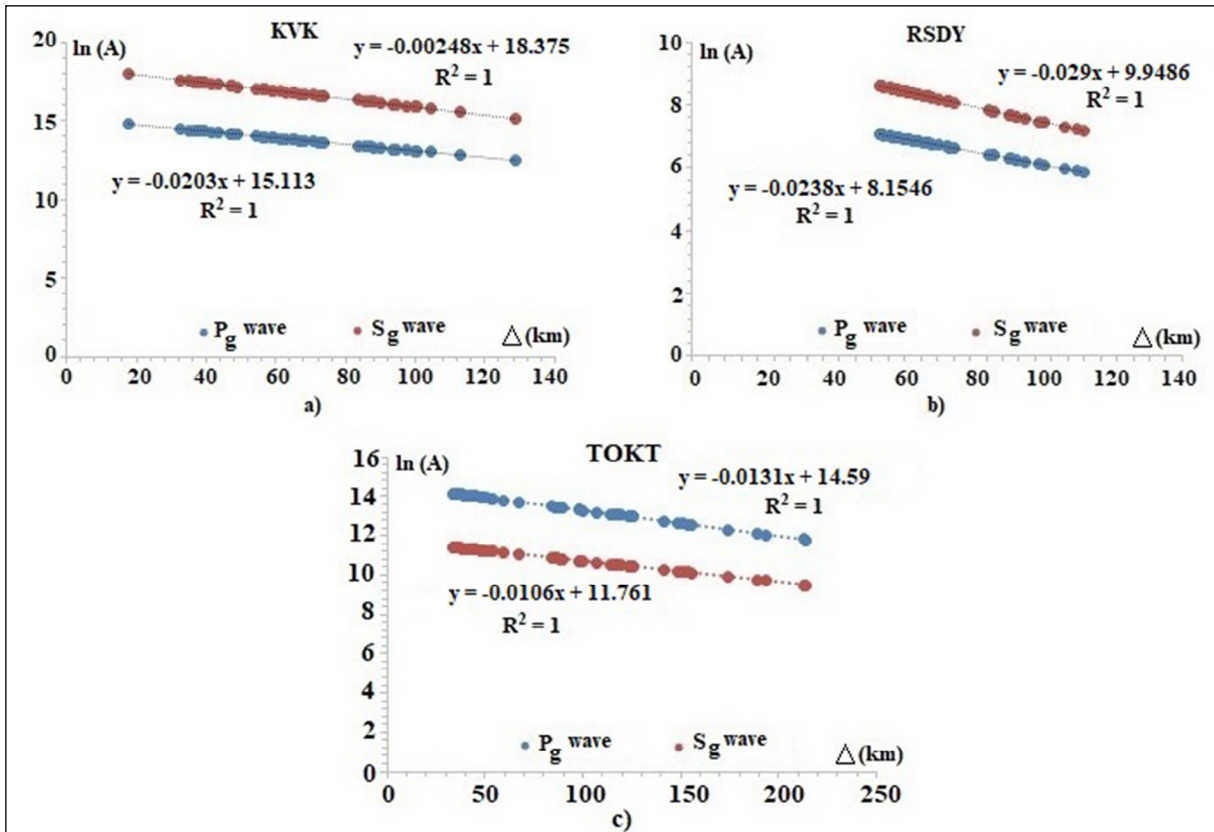


Figure 8- $\ln(A) - \Delta$ (km) graphs and $P_g - S_g$ absorption values of the stations; a) KVK, b) RSDY and c) TOKT.

it is observed that the TOKT station is located in the stress relaxation region caused by the 9th October 2015 earthquake, while RSDY and KVK stations are outside the impact area.

6. Results

According to the stress and strain values calculated with the Coulomb software using the earthquake focal mechanism solutions values of the 9th October 2015 Yoldere-Erbaa (Tokat) ($M_L = 5.1$) earthquake, the shear, normal, and Coulomb stress values are changing between $-0.01 - 0.01$ bars. The XX, YY and ZZ components of the strain values have values ranging from $-1 \cdot 10^8$ to $1 \cdot 10^8$. As a result, the amplitude of the stresses and strains caused by the earthquake are generally low in and around the region where the earthquake occurred.

The δp absorption coefficients ranging from 0.01 to 0.03 and δs absorption coefficients ranging from 0.0135 to 0.025 of the lateral tomography of

the study area. According to the regional absorption coefficients, it can be said that the stress accumulation surrounding and under the crust of the TOKT station, where the absorption was the least, are greater than the other two stations. It can be deduced that pressure is accumulated, particularly around the MOFZ and EPFZ and their surroundings.

While the velocity is 20 mm per year for NAFZ and its surroundings, it is far below 20 mm per year at sites (SAM1, FASA, GIRS) located in the north of the NAFZ. The fact that the stations located in the north of the NAFZ (SAM1, FASA, GIRS) have slower velocities than the others (VEZI, RDIY, CORU, TOK1) can be obtained with the effect of the sense of NAFZ (right-lateral strike-slip fault).

Acknowledgements

This research was conducted as part of the Atatürk University Scientific Research Projects (Project No: 8443), which was a collaborative effort between

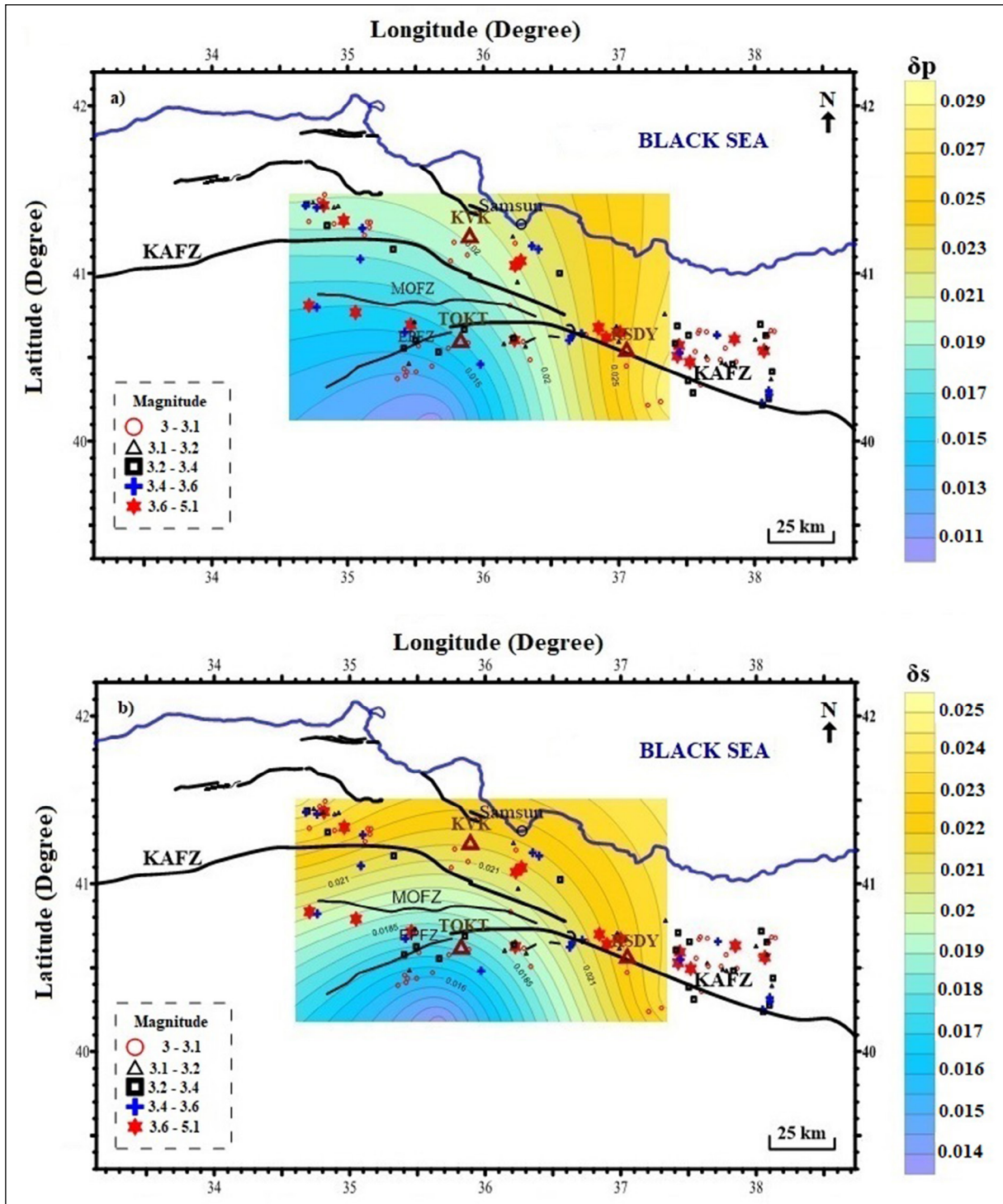


Figure 9- Obtained from the station; a) $\delta\rho$ regional absorption coefficients, and b) the lateral tomography of $\delta\sigma$ regional absorption coefficients. NAFZ: North Anatolian Fault Zone, MOFZ: Merzifon Ovacık Fault Zone, EPFZ: Ezinepazarı Fault Zone.

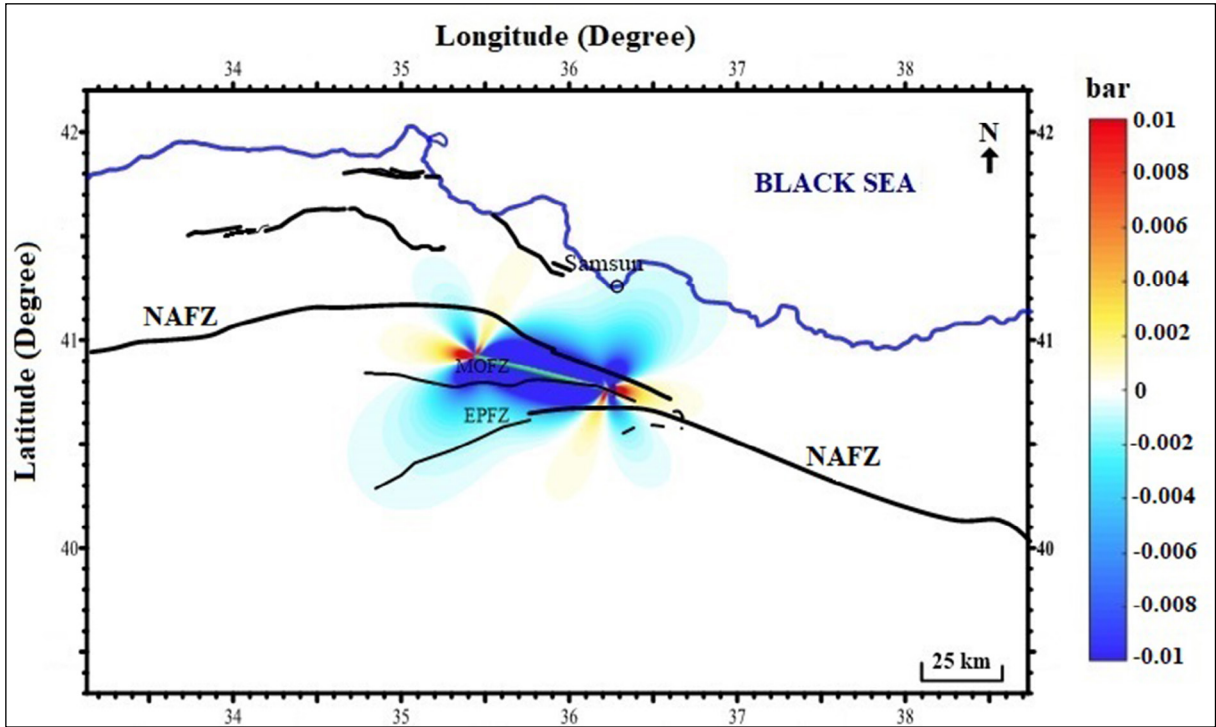


Figure 10- Coulomb stress changes on the study field. NAFZ: North Anatolian Fault Zone, MOFZ: Merzifon Ovacık Fault Zone, EPFZ: Ezinepazarı Fault zone.

Atatürk University and Dokuz Eylül University. GNSS data used in the study were provided from the CORS-TR system is operated by the General Directorate of Maps and the General Directorate of Land Registry and Cadastre. Generic Mapping Tools (GMT) were used to create some figures (Wessel et al., 2019). We'd like to express our gratitude to the three referees for their time and participation in the article's development.

References

- Affandi, A. K., Sailah, S., Ardiansyah, S., Wafiazizi, M. 2019. An analysis of Coulomb stress change and triggering interaction toward seismic activities in the area West Sumatera within January 2000 - June 2018. *Journal of Physics, Conference Series*, 1282.
- Aki, K. 1969. Analysis of the seismic coda of local earthquakes as scattered waves. *Journal of Geophysical Research* 74(2), 615-631.
- Aki, K., Chouet, B. 1975. Origin of coda waves: source, attenuation, and scattering effects. *Journal of Geophysical Research* 80(23), 3322-3342.
- Aki, K., Richards, P. G. 1980. *Quantitative Seismology: Theory and Methods*. Freeman, San Francisco.
- Arpat, E., Şaroğlu, F. 1975. Türkiye'deki bazı önemli genç tektonik olaylar. *Türkiye Jeoloji Kurumu Bülteni* 18(1), 91-101.
- Aydın, U. 2011. Erzincan - Muş - Oltu (Erzurum) arasındaki yüzey kayaların soğurma özelliklerinin incelenmesi. *Doktora Tezi, Çukurova Üniversitesi, Fen Bilimleri Enstitüsü*, 136, Adana.
- Aydın, U. 2014. Crustal stresses and seismodynamic characteristics in the upper crust. *Open Journal of Earthquake Research* 3(04), 143.
- Aydın, U. 2016. Relationships between geotectonic and seismodynamic characteristics of the crust in the Eastern Anatolia. *Acta Geodaetica et Geophysica* 51(1), 69-79.
- Aydın, U., Kadirov, A. 2008. Erzincan ve çevresinde P dalgası soğurulması. *Sakarya Üniversitesi Fen Bilimleri Enstitüsü Dergisi* 12(1), 1-8.
- Chinnery, M. 1963. The stress changes that accompany strike - slip faulting. *Bulletin of the Seismological Society of America* 53(5), 921-932.
- Chopra, S., Alexeev, V. 2004. A new approach to enhancement of frequency bandwidth of surface seismic data. *First Break* 22(8).
- Çırmık, A. 2014. Determining the deformations in Western Anatolia with GPS and gravity measurements.

- Doktora Tezi, Dokuz Eylül Üniversitesi, Fen Bilimleri Enstitüsü, 196, İzmir.
- Çırmık, A., Pamukçu, O. 2017. Clarifying the interplate main tectonic elements of Western Anatolia, Turkey by using GNSS velocities and Bouguer gravity anomalies. *Journal of Asian Earth Sciences* 148, 294-304.
- Çırmık, A., Özdağ, O. C., Doğru, F., Pamuk, E., Gönenç, T., Pamukçu, O., Akgün, M., Arslan, A. T. 2016. The soil behaviors of the GNSS station. *Earth Sciences* 5(5), 70.
- Çırmık, A., Doğru, F., Gönenç, T., Pamukçu, O. 2017. The stress/strain analysis of kinematic structure at Gülbahçe Fault and Uzunkuyu Intrusive (İzmir, Turkey). *Pure and Applied Geophysics* 174(3), 1425-1440.
- Harris, R. A., Simpson, R. W. 1992. Changes in static stress on southern California faults after the 1992 Landers earthquake. *Nature* 360(6401), 251-254.
- Herring, T. A., King, R. W., Floyd, M. A., McClusky, S. C. 2015. Introduction to GAMIT/GLOBK, Release 10.6., Massachusetts Institute of Technology, Cambridge.
- KOERI (Boğaziçi University Kandilli Observatory Earthquake Research Institute, Kandilli Rasathanesi Deprem Araştırma Enstitüsü). 2021. 09 Ekim 2015 Yoldere-Erbaa (Tokat) Depremi. <http://www.koeri.boun.edu.tr/sismo/2/wp-content/uploads/2015/10/09-Ekim-2015-Yoldere-Erbaa-Tokat-Depremi-1.pdf>. 1 Mart 2021.
- Ketin, I. 1948. Über die tektonisch-mechanischen Folgerungen aus den grossen anadoluischen Erdbeben des letzten Dezenniums. *Geologische Rundschau* 36(1), 77-83.
- Koçyiğit, A., Yılmaz, A., Adamia, S., Kuloshvili, S. 2001. Neotectonics of East Anatolian Plateau (Turkey) and Lesser Caucasus: implication for transition from thrusting to strike-slip faulting. *Geodinamica Acta* 14(1-3), 177-195.
- Okada, Y. 1992. Internal deformation due to shear and tensile faults in a half-space. *Bulletin of Volcanology* 47, 239-246.
- Pamukçu, O., Gönenç, T., Çırmık, A., Sındırgı, P., Kaftan, I., Akdemir, Ö. 2015. Investigation of vertical mass changes in the south of İzmir (Turkey) by monitoring microgravity and GPS/GNSS methods. *Journal of Earth System Science* 124(1), 137-148.
- Stein, R. S., King, G. C., Lin, J. 1992. Change in failure stress on the southern San Andreas fault system caused by the 1992 magnitude= 7.4 Landers earthquake. *Science* 258(5086), 1328-1332.
- Şaroğlu, F., Emre, Ö., Boray, A. 1987. Türkiye'nin diri fayları ve depremsellikleri. Maden Tetkik ve Arama Genel Müdürlüğü, Rapor No: 8174, Ankara.
- Şengör, A. 1979. The North Anatolian transform fault: its age, offset and tectonic significance. *Journal of the Geological Society* 136(3), 269-282.
- Şengör, A. C., Natal'in, B. A. 1996. Turcic-type orogeny and its role in the making of the continental crust. *Annual Review of Earth and Planetary Sciences* 24(1), 263-337.
- Şengör, A., Tüysüz, O., İmren, C., Sakıncı, M., Eyidoğan, H., Görür, N., Le Pichon X., Rangin, C. 2005. The North Anatolian fault: a new look. *Annual Review of Earth and Planetary Sciences* 33, 37-112.
- Taymaz, T., Jackson, J., McKenzie, D. 1991. Active tectonics of the north and central Aegean Sea. *Geophysical Journal International* 106(2), 433-490.
- Toda, S., Stein, R. S., Sevilgen, V., Lin, J. 2011. Coulomb 3.3 graphic-rich deformation and stress-change software for earthquake, tectonic, and volcano research and teaching-user guide. US Geological Survey Open - file report: 1060(2011), 63.
- Toksöz, M. N., Johnston, D. H. 1981. *Seismic Wave Attenuation*. Society of Exploration Geophysicists, Tulsa, Okla, 2.
- Ugalde, A., Carcolé, E., Vargas, C. A. 2010. S-wave attenuation characteristics in the Galeras volcanic complex (southwestern Colombia). *Physics of the Earth and Planetary Interiors* 181(3-4), 73-81.
- Wessel, P., Luis, J. F., Uieda, L., Scharroo, R., Wobbe, F., Smith, W. H. F., Tian, D. 2019. The generic mapping tools version 6. *Geochemistry, Geophysics, Geosystems* 20, 5556-5564.

